



# 1 Karst spring recession curve analysis: efficient, accurate methods for 2 both fast and slow flow components

3

4 Tunde Olarinoye<sup>1</sup>, Tom Gleeson<sup>2</sup>, Andreas Hartmann<sup>1,3</sup>

5 <sup>1</sup>Chair of Hydrological Modeling and Water Resource, University of Freiburg, Germany

6 <sup>2</sup>Department of Civil Engineering, University of Victoria, BC, Canada

7 <sup>3</sup>Department of Civil Engineering, Bristol University, UK

8

9 *Correspondence to:* Tunde Olarinoye (tunde.olarinoye@hydmod.uni-freiburg.de)

## 10 **Abstract.**

11 Analysis of karst spring recession hydrographs is essential for determining hydraulic parameters, geometric characteristics and  
12 transfer mechanisms that describe the dynamic nature of karst aquifer systems. The extraction and separation of different fast  
13 and slow flow components constituting karst spring recession hydrograph typically involve manual and subjective procedures.  
14 This subjectivity introduces bias, while manual procedures can introduce errors to the derived parameters representing the  
15 system. To provide an alternative recession extraction procedure that is automated, fully objective and easy to apply, we  
16 modified traditional streamflow extraction methods to identify components relevant for karst spring recession analysis.  
17 Mangin's karst-specific recession analysis model was fitted to individual extracted recession segments to determine matrix  
18 and conduit recession parameters. We introduced different parameters optimisation approaches of the Mangin's model to  
19 increase degree of freedom thereby allowing for more parameters interaction. The modified recession extraction and  
20 parameters optimisation approaches were tested on 3 karst springs in different climate conditions. The results show that the  
21 modified extraction methods are capable of distinguishing different recession components and derived parameters reasonably  
22 represent the analysed karst systems. We recorded an average KGE >0.7 among all recession events simulated by recession  
23 parameters derived from all combinations of recession extraction methods and parameters optimisation approaches. While  
24 there are variability among parameters estimated by different combinations of extraction methods and optimisation approaches,  
25 we find even much higher variability among individual recession events. We provide suggestions to reduce the uncertainty  
26 among individual recession events and to create a more robust analysis by using multiple pairs of recession extraction method  
27 and parameters optimisation approach.

## 28 **1 Introduction**

29 Groundwater from karst aquifers are essential water sources globally (Stevanović 2018; Goldscheider et al. 2020). Karst  
30 aquifers are characterised by high degree of heterogeneity and complex flow dynamics resulting from the interplay of conduit  
31 and matrix drainage systems (Király 2003; Goldscheider and Drew 2007). Groundwater flow is rapid in the highly-conductive



32 conduit system whereas it is several order of magnitude slower in the less-conductive matrix system (Goldscheider 2015).  
33 While both systems have significant storage capacities, groundwater residence time is longer in the matrix than the conduit  
34 system (Kovács et al. 2005).

35

36 Several methods including detailed site-specific speleological investigation (Ford and Williams 2007), tracer tests  
37 (Goldscheider and Drew 2007; Goldscheider and Neukum 2010), hydrograph analysis (Kovács et al. 2005; Fiorillo 2014) and  
38 model ensembles (Fandel et al. 2020) are used to characterize groundwater flow dynamics in karst systems. Aside from  
39 hydrograph analysis which usually requires only spring discharge time series data, other methods are either expensive to apply,  
40 time consuming or require more input, thus making time series a commonly applied method for karst aquifer flow analyses  
41 and modelling (Ford and Williams 2007).

42

43 Quantitative time series analysis provides a lumped attributes of an entire karst aquifer system that are rather difficult to directly  
44 measure (Kovács et al. 2005). Karst spring recession analysis still remains a vital quantitative time series analysis tool for  
45 estimating aquifer parameters and geometric properties (Fiorillo 2011). Discharge from karst springs reflects the complex  
46 interplay of conduit and matrix systems, and provides insight about the characteristics of the aquifer which sustains the spring  
47 (Kovács et al. 2005; Fiorillo 2014). This also provide essential information for flow prediction as the shape of spring  
48 hydrograph reflects variable aquifer responses to different recharge pathways (Ford and Williams 2007). Since the shape of  
49 the spring hydrograph describe in an integrated manner how different aquifer storages and processes control the spring flow  
50 (Jeannin and Sauter 1998; WMO 2008a), analysing individual recession limbs of spring hydrograph therefore offers extensive  
51 understanding into the structural, storage and behavioral dynamics of the karst system's drainage (Bonacci 1993).

52

53 Numerous studies have employed recession analyses of karst spring hydrograph to characterise karst aquifers, evaluate aquifer  
54 properties, manage groundwater resources, predict low flow and estimate baseflow parameters (Padilla et al. 1994a; Dewandel  
55 et al. 2003; Kovács et al. 2005; Fiorillo 2014). Derived or estimated recession coefficients are also important parameters in  
56 karst models for simulating rainfall-discharge (Fleury et al. 2007; Mazzilli et al. 2019) and other process-based modelling  
57 (Hartmann et al. 2013, 2014).

58

59 Unlike porous media, karst systems cannot be represented by one single storage-discharge function (Ford and Williams 2007).  
60 They comprise of multiple subsystems of interconnected conduit and matrix reservoirs, each with their own storage-discharge  
61 characteristics (Jeannin and Sauter 1998). Recession analysis models specifically developed for karst spring analysis are thus  
62 comprised of two (Mangin 1975) or more (Fiorillo 2011; Xu et al. 2018) independent storage-discharge transfer functions to  
63 describe drainage characteristics of different reservoirs and simulate recession flows. Dewandel et al. (2003) provide general



64 overview and main characteristics of commonly used recession models and those specifically applied to karst systems.  
65 Separating the conduit (quickflow) and matrix (slowflow) components of karst spring recession curve is key in correctly  
66 applying and fitting the recession models. Extracting these components is done through a semi-logarithmic plot that usually  
67 reveals two or more segments. At least one of these segments, which is typically the last, represents linear reservoir drainage  
68 and it is attributed to the matrix component (Bonacci 1993; Ford and Williams 2007). However, this extraction approach is  
69 manually and subjectively applied resulting to imprecise and inconsistent estimations. The amount of time required to manually  
70 fit a straight line and identify the matrix component also makes it impractical to apply this approach to large number of  
71 hydrographs or multiple recession curves.

72

73 While a handful of automated recession extraction routines have been developed for extracting streamflow recessions  
74 (Arciniega-Esparza et al. 2017), these approaches, based on different statistical indices to detect less variable flow conditions  
75 are explicitly used to extract the baseflow recession. During baseflow, streamflow is supported by groundwater and storage  
76 reservoirs which provide a less variable flow condition. Contributions from runoff and other unregulated sources that produce  
77 high variable flow during quickflow recession are discarded by the extraction routine (Vogel and Kroll 1996; Brutsaert 2008).

78

79 However, these recession extraction routines developed for streamflow could be adapted to extract conduit and matrix flow  
80 recession of karst springs. Since these routines are developed to identify baseflow (matrix) component of streamflow (karst  
81 spring flow) recessions and discard the quickflow (conduit) component, we can modify it to identify the quickflow as well  
82 rather than discarding them. But as these routines are based on different statistical indices for identifying the baseflow regime,  
83 they perform differently and could produce differing recession parameters (Stoelzle et al. 2013; Santos et al. 2019).

84

85 The objective of this study is to develop and test a robust and objective approach to extract karst spring recession components  
86 as well as derive parameters associated with the different components of karst drainage systems. Therefore, in this study we:

87

88 • Develop automated karst recession extraction methods that can identify conduit and matrix component of karst spring  
89 recession hydrograph by adapting and modifying different baseflow recession extraction routines for streamflow.

90

91 • Estimate conduit and matrix drainages recession parameters of sample springs using the combination of different modified  
92 extraction methods and parameters optimisation approaches of karst recession model.

93



94 • Evaluate the performance of the different combinations of modified extraction procedures and karst recession model  
95 parameters optimisation approaches by comparing the ranges and distribution of recession parameters, efficiency measures  
96 and spring characterisations.

97

98 For this study, the recession parameters are estimated by fitting the karst recession model to individual recession segments  
99 extracted by the extraction methods. Unlike master recession curve, analysis of individual recession segments allows to  
100 explicitly account for variability in the individual recession events resulting from different input (precipitation) and other initial  
101 conditions (WMO 2008b).

## 102 **2 Data and Methods**

103 To develop an automatic karst-specific recession extraction and analysis procedure that is objective and applicable to large  
104 hydrograph samples, we first explore the applicability of generic recession extraction procedures originally developed for non-  
105 karst streamflow recessions (Vogel and Kroll 1992; Brutsaert 2008; Aksoy and Wittenberg 2011). Then we analyse karst  
106 recession parameters using two-parallel drainage recession model was used to simulate recession curves (Mangin 1975). In  
107 the following subsections, we described the recession extraction and analysis model, parameters optimisation approaches, as  
108 well as the various adaptations and modifications implemented. For consistency, we use the terms ‘quick flow’ for the turbulent  
109 flow from highly conductive karst drainage pathways (synonymous with conduit and storm flow) and ‘slow flow’ for the  
110 laminar flow contribution from less conductive fissures and pores (synonymous with matrix, diffuse and base flow) (Atkinson  
111 1977; Larson and Myroie 2018).

### 112 **2.1 Adapting streamflow methods to extract matrix and conduit recession components**

113 We adapt three different streamflow recession methods (Vogel and Kroll 1992; Brutsaert 2008; Aksoy and Wittenberg 2011)  
114 to extract matrix and conduit recession components (Table 1), herein called recession extraction methods (REMs). Vogel and  
115 Kroll (1992) developed an automated base flow recession extraction routine for streamflow. A 3-day moving average is firstly  
116 apply to smoothing the hydrograph, and the decreasing segments of the 3-day moving average are selected as the recession  
117 hydrograph. Only segments with 10 or more consecutive days are recognised as recession candidates. To exclude surface and  
118 storm runoff influence at the beginning of recession, the first 30% of each recession segment is deleted. Additionally, the  
119 difference between two consecutive streamflow values must be  $\leq 30\%$  for the pairs to be accepted. All recession segments that  
120 satisfy these conditions are then accepted as base flow (non-influenced) recessions segment.

121

122 In order to objectively determine streamflow recession that is derived purely from a dry or low flow period, Brutsaert (2008)  
123 introduced more strict recession extraction method. For streamflow  $Q$ , during time  $t$ , the Brutsaert method eliminates data



124 point with increased or zero values of  $dQ/dt$ , as well as points with abrupt  $dQ/dt$  values. To exclude data points that might be  
125 influenced by storm runoff, three data points after a positive or zero  $dQ/dt$  are removed; in majors events, an additional fourth  
126 data point is removed. While Brutsaert (2008) did not provide a description for a majors event, Stoelzle et al. (2013) applied  
127 the Brutsaert method in their study and defined major event as streamflow values exceeding 30% streamflow frequency.  
128 Therefore, our study uses this definition of major event from Stoelzle et al. (2013). Furthermore, the Brutsaert method also  
129 excludes last two data points before a positive or zero  $dQ/dt$  and spurious data points with larger  $-dQ/dt$  values.

130

131 Aksoy & Wittenberg (2011) extracted the baseflow component from daily streamflow hydrograph during recession by  
132 comparing the coefficient of variation (CV) of the recession segment. All days with decreasing or equal observed flowrate  
133 observations are considered as part of the recession curve. Subsequently, a non-linear reservoir model (Eq. 1) is iteratively  
134 fitted to the recession curve until the CV is  $\leq 0.1$ . The CV is defined as the ratio of standard deviation between observed  
135 flowrates measurements (Qs) and calculated flowrate (Qcalc) to the mean of the observed flowrates as expressed by Eq. 2.  
136 Segment of the recession curve with the  $CV \leq 0.1$  is selected as the real baseflow recession, otherwise excluded. Only recession  
137 curves with 5-day periods or longer are considered. If the number of days becomes less than 5 during iterative curve fitting  
138 and  $CV \leq 0.1$  is not achieved, such recession event is discarded (Aksoy and Wittenberg 2011).

139

140

$$141 \quad Q_t = Q_0 \left[ 1 + \frac{(1-b)Q_0^{1-b}}{ab} \right]^{\frac{1}{b-1}} \quad (1)$$

142

143

$$144 \quad CV = \sqrt{\frac{n^2 \sum(Q - Q_{calc})^2}{n-1 \sum(Q)^2}} \quad (2)$$

145

146 The three recession extraction approaches (Vogel and Kroll 1992; Brutsaert 2008; Aksoy and Wittenberg 2011) were  
147 specifically developed to extract streamflow recessions that are mainly from baseflow contribution. Thus, rule based and  
148 exclusion criteria specified by each method ensure that quick flow influences were eliminated from extracted recession  
149 segments. In karst systems concentrated rapid flow through the conduit networks constitutes the quick flow, while the  
150 contribution from slow-velocity drains through the matrix pores constitutes the slow flow (baseflow). The quick and slow flow  
151 represents flows from two different drainage structures and both contribute to karst spring recession (Fiorillo, 2014; Ford &  
152 Williams, 2007; Padilla et al., 1994).

153



154 Adapting streamflow methods for karst spring recession analysis requires both slow and fast flow components to model matrix  
 155 and conduit spring discharges, so we (i) extract spring flow recession curve based on the specific method approach, (ii) attribute  
 156 part of the recession curve that satisfies the specified method's exclusion criteria as slow flow (matrix) component, and (iii)  
 157 assign the remaining part that is excluded as quick flow (conduit) component. Table 1 provides an overview of the rule-based  
 158 baseflow recession extraction methods and changes made in adapting them to include quickflow component of recession.  
 159

160 Table 1: Criteria for recession extraction methods (REMs)

	Extraction method	General Criteria	Filter	Slow flow selection	Adaptation for Quick flow selection
Vogel	Vogel and Kroll (1992)	Decreasing 3-day moving day average	First 30% days	$\frac{Q_i - Q_{i+1}}{Q_{i+1}} \leq 30\%$	First 30% days, $\frac{Q_i - Q_{i+1}}{Q_{i+1}} \geq 30\%$
Brutsaert	Brutsaert (2008)	$\frac{dQ}{dt} < 0$	First 3 or 4, and last 2 days		First 3 or 4 days
Aksoy	Aksoy and Wittenberg (2011)	$\frac{dQ}{dt} \leq 0$	-	$CV \leq 0.10$	$CV \geq 0.10$

161

## 162 2.2 Karst recession analysis model

163 After extraction, we apply Mangin's (1975) recession analysis model which has been widely used for estimating drainage  
 164 characteristics and aquifer dynamics in fractured non-homogeneous media (Fleury et al. 2007; Liu et al. 2010; Xu et al. 2018;  
 165 Schuler et al. 2020; Sivelles 2020). To analyse the extracted recessions, we use this method which considers a two-component  
 166 recession curve by distinguishing between quick flow (mostly through karstic conduits) and slow flow (mostly through the  
 167 fissure matrix of the carbonate rock) recessions (Figure 1). Mangin presented two equations: Eq.3 describes the linear storage-  
 168 discharge relationship from the saturated zone during slowflow condition represent by the Maillet (1905) equation.

169

170 
$$\phi_t = Q_{r0} e^{-\alpha t} \quad (3)$$

171



172 where  $Q_{ro}$  is the baseflow contribution at the beginning of recession when  $t = 0$ ,  $\alpha$  is the recession coefficient with a unit of  $T^{-1}$   
173 and  $t$  is the lapsed time between discharge at any time  $t$ ,  $Q_t$  and initial discharge at  $t = 0$ ,  $Q_0$ ; and Eq. 4 describes the non-  
174 linear relationship during quickflow recession from the unsaturated zone.

175

$$176 \quad \Psi_t = q_0 \frac{1-\eta t}{1+\varepsilon t} \quad (4)$$

177

178 where  $q_0$  is the difference between  $Q_0$  and  $Q_{ro}$ , parameter  $\eta$  describes the infiltration rate through the unsaturated zone. The  
179 parameter is defined as  $1/t_i$  for the duration of quickflow recession between  $t = 0$  and  $t_i = 1/\eta$ .  $\varepsilon$  in  $T^{-1}$  unit describes the  
180 regulating capacity of the unsaturated zone during infiltration and characterises importance of concavity of quickflow recession  
181 (Padilla et al. 1994). The algebraic sum of Eq. 3 and 4 gives Eq. 5, which defines the discharge at time  $t$  during the recession  
182 period.

183

$$184 \quad Q_t = \Phi_t + \Psi_t \quad (5)$$

185

186 Since  $t_i$  is the point of intersection of slowflow and quickflow component of the recession curve and infiltration stopped when  
187  $t > t_i$  ( $t > 1/\eta$ ), so the quickflow component  $\psi_t$  in Eq. 5 is essentially assumed to be zero at that point ( $\psi_t = 0$ ) (Ford and Williams  
188 2007; Civita and Civita 2008). Therefore, the application of the Mangin's model require, firstly fitting the slowflow component  
189  $\phi_t$ , to the slowflow segment of recession curve using Eq. 3 to determine the recession coefficient  $\alpha$ . Afterwards, Eq. 5 is then  
190 fitted to determine the  $\eta$  and  $\varepsilon$  parameters of the quickflow segment. However, the accuracies of  $Q_{ro}$ ,  $t_i$  and the linear  
191 representativeness of the slowflow component of the recession curve is critical for the reliable estimation of recession  
192 coefficients (Ford and Williams 2007). Also the dynamic volume,  $V_{dyn}$ , which is defined as the volume of water stored in the  
193 aquifer during depletion of spring discharge is estimated with Eq. 6.

194

$$195 \quad V_{dyn} = \frac{Q_{ro}}{\alpha} \quad (6)$$

196

197 Additionally, Mangin introduced five classes of karst system based on two parameters that are calculated using the recession  
198 parameters: (1) the aquifer regulation capacity,  $K$ , defined as ratio between dynamic aquifer volume,  $V_{dyn}$ , and observed volume  
199 of discharge,  $V_{ann}$ , through the spring in one hydrological year (Eq. 7);

200



201  $K = \frac{V_{dyn}}{V_{ann}}$  (7)

202

203 and (2) infiltration delay,  $i$ , given by Eq. 8 which is calculated as the value of the quickflow recession component after two  
 204 days ( $t=2$ ).

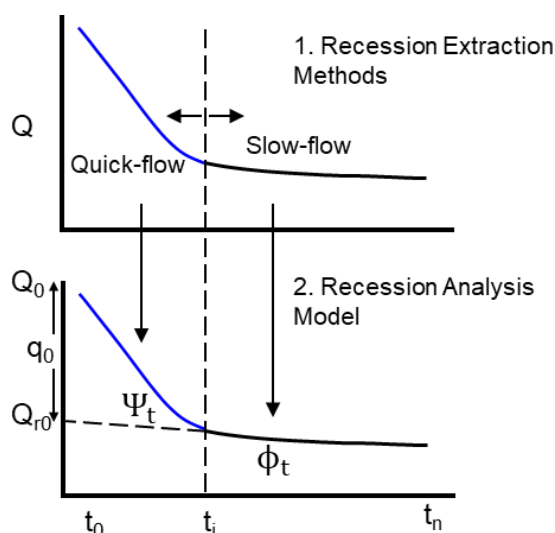
205

206  $i = \frac{1-\eta t}{1+\epsilon t}$  (8)

207

208 Ford and Williams (2007) provided a detailed review of karst aquifer recession analysis and application of the Mangin model.

209



210

211 Figure 1. An illustration of karst spring recession curve showing separation into linear and non-linear components by recession extraction  
 212 method and fitting appropriate components of recession analysis model.

### 213 2.3 Estimation of recession parameters

214 Recession parameters can be derived by: (i) considering accumulation of all extracted recession events, a so-called “master  
 215 recession”, and (ii) estimating multiple parameter combinations from individual recession event. In a recent study, Jachens et  
 216 al., (2020) recommended avoiding the former approach as its estimated parameters do not represent average catchment  
 217 responses nor their variability. For this study, the parameters are estimated for individual, automatically extracted recession  
 218 events. That way, we capture variability of spring discharge across individual recharge events (Jachens et al. 2020). As  
 219 mentioned in subsection 2.2, in the standard Mangin’s approach, the slowflow component of the recession curve (Eq. 3) is  
 220 fitted at first to determine  $\alpha$ . Also, the  $\eta$  parameter of the quickflow component (Eq. 4) which is equivalent to  $1/t_i$  is  
 221 predetermined, meaning that quick flow abruptly ends at  $t_i$  days, which in reality is actually untrue. Hence, reliable





222 determination of  $t_i$  through the extraction routines (REMs) is vital for estimation of recession parameters. These standard  
223 procedures involve with the application of Mangin's model result in less degree of freedom for parameter interaction and  
224 unrealistic abrupt ending of quick flow after  $t_i$  days. To increase the degree of freedom and assess the importance of  $t_i$  and the  
225 effect of a priori estimated  $\eta$  ( $1/t_i$ ) on the Mangin's recession model, we introduced three optimization approaches which are  
226 referred to as three different parameters optimisation approaches (POAs) used in this study.

227

228 • **M1:** This follows the standard approach for applying the Mangin model as described by Padilla et al (1994) and Ford  
229 and Williams (2007). The slowflow component of the recession curve is fitted first with Eq. 3 for  $t_i \leq t \leq t_n$  to determine  
230  $\alpha$  value while the quickflow component is assumed to be zero during this period. Afterwards, the second parameter  
231  $\varepsilon$  is optimised by fitting the quickflow component with Eq. 5 using a predefined value of  $\eta$  parameter ( $\eta = 1/t_i$ ) for the  
232 event duration between  $t_0 \leq t < t_i$ .

233

234 • **M2:** The conventional approach for fitting the Mangin model (M1) does not provide for independent or flexible  
235 estimation of  $\eta$ . The prior definition of  $\eta$  as  $1/t_i$  rely on the accuracy of the extraction method to detect the point of  
236 inflexion  $t_i$ . This however does not give the flexibility to optimised  $\eta$  to a value that could provide better fit for the  
237 model. To provide for more flexible estimation of  $\eta$ ,  $\alpha$  parameter is determined as in M1, then Eq. 5 is fitted to the  
238 complete segment of recession curve for  $t_0 \leq t \leq t_n$  to determine best values of  $\varepsilon$  and  $\eta$  parameters.

239

240 • **M3:** This is a very flexible approach that allows for  $\alpha$ ,  $\varepsilon$ ,  $\eta$  and  $Q_{ro}$  values to be fitted numerically. The determination  
241 of  $t_i$  and  $Q_{ro}$  does not depend on the extraction method, rather the best fit for the parameters are obtained from  
242 optimisation process. The Mangin model (Eq. 5) is fitted to entire recession curve, which allows for absolute  
243 flexibility of  $t_i$  and robust parameters interaction during optimisation. With the model calibrated  $t_i$  ( $1/\eta$ ), separating  
244 the quick- and slowflow segments now entirely rely on the optimisation exercise rather than extraction techniques.

245

246 For the optimisation exercise, a non-linear least squares procedure with spring discharge records was used. To avoid having  
247 negative value of conduit drainage contribution when the optimised  $t_i$  ( $1/\eta$ ) is greater than the elapsing  $t$  value, the quick flow  
248 component,  $\psi_t$  (Eq. 4), is constrained to a minimum value of zero. Table 2 provides summary of the different optimisation  
249 approaches, parameters that were optimised as well as duration of the optimised corresponding flow component.

250

251 Table 2: Optimised recession parameters for the three different parameters optimisation approaches (POAs) of the Mangin recession analysis  
252 model.

Optim.	Optimized	Condition	Slowflow	Quickflow	Degree of
--------	-----------	-----------	----------	-----------	-----------



approach	parameters	component	component	freedom	
M1	$\alpha, \varepsilon$	$\eta = 1/t_i$	$t_i \leq t \leq t_n$	$t_0 \leq t \leq t_i$	Less flexible
M2	$\alpha, \varepsilon, \eta$	$\eta \neq 1/t_i$	$t_i \leq t \leq t_n$	$t_0 \leq t \leq t_n$	Intermediate
M3	$\alpha, \varepsilon, \eta, Q_{ro}$	$\eta \neq 1/t_i$	$t_0 \leq t \leq t_n$	$t_0 \leq t \leq t_n$	Very flexible

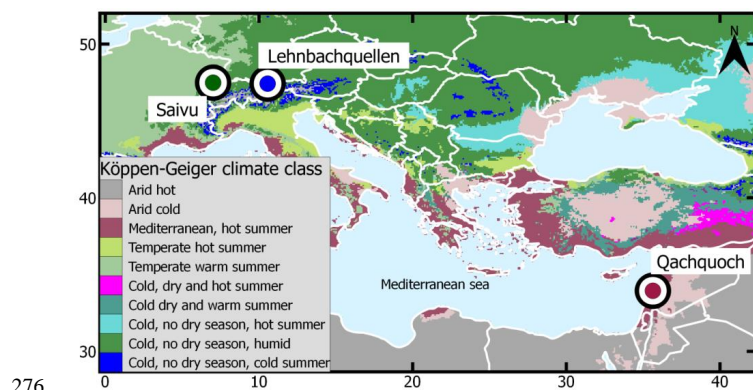
253

254 **2.4 Comparison and evaluation of REMs and POAs**

255 The three REMs (Vogel, Brutsaert and Aksoy) are combined with the three POAs (M1, M2 and M3) of the recession model  
 256 to derive slow and quick flow recession parameters of selected karst springs for a total of nine possible methods. The mean  
 257 and interquartile ranges of the derived parameters are compared among different method pairs and individual recession events.  
 258 Models performance is determined by calculating goodness of fit between observed spring recession discharges and ones  
 259 simulated with the derived parameters using Kling Gupta Efficiency (KGE) measures (Gupta et al. 2009). The estimated  
 260 recession parameters were used to identify the dynamic of the systems according to Mangin’s karst system classification  
 261 described in subsection 2.2. The Mangin classification scheme describes the aquifer drainage characteristics, conduit  
 262 development and speleological network (Mangin 1975; El-Hakim and Bakalowicz 2007). Therefore, this is use to evaluate the  
 263 representativeness of recession parameters estimated for the selected karst springs aquifer systems.

264 **3 Test springs and data**

265 The REMs and POAs were tested using three karst springs; Lehnbachquellen, Saivu and Qachquoch located in Austria,  
 266 Switzerland and Lebanon respectively (Figure 2). The selection of these springs were based on geographical spread which  
 267 covers different climate and hydrological settings, availability of discharge hydrograph in high resolution as well as literature  
 268 reference on hydrological characterisation of aquifer systems drained by the spring. Daily and sub-daily spring discharge time  
 269 series of the selected springs were obtained from WoKaS database (Olarinoye et al. 2020). Important characteristics of the  
 270 spring hydrographs as well as the catchments in which they are sited are presented in (Table 3). The springs are sited in  
 271 catchments distinguished by different climate conditions according to the Köppen-Gieger classification (Beck et al. 2018).  
 272 Lehnbachquellen is sited in snow-dominated, Saivu in humid and Qachquoch is in the Mediterranean catchment. The spring  
 273 discharge time series measured at a uniform time-step for each spring span between 3 and 13 years. All discharge time series  
 274 were aggregated to daily temporal resolution and missing data values which were only found (<0.01%) in Lehnbachquellen  
 275 spring discharge data were excluded.



276

277 Figure 2. Map showing locations of the three test springs obtained from the WoKaS database and different Köppen-Geiger hydroclimatic  
 278 classes.

279 Table 3. Summary of test springs site properties and characteristics of spring discharge hydrographs.

Properties	Lehnbachquellen	Saivu	Qachquoch
Climate description	Snow-dominated	Humid	Mediterranean
Spring elevation (masl)	1293	371	65
Köppen-Geiger	Cold and no dry season	Cold and humid	Mediterranean, hot summer
Temporal res.	Daily	Hourly	Sub-hourly
Length	1999-2012	1993-1995	2014-2018
Missing data	<0.01%	0	0
Mean discharge (m <sup>3</sup> /s)	0.06	0.29	1.08
Mean precipitation (mm/y)	1396	1201	523

280

## 281 4 Results

### 282 4.1 Extracted recessions and performance of POAs

283 The adapted recession extraction methods adequately identify karst spring conduit and matrix flow components and the  
 284 parameters obtained with the fitted Mangin's models produce a well satisfactory recession simulation. The combination of the  
 285 three REMs (Vogel, Brutsaert and Aksoy) and three POAs (M1, M2 and M3) led to nine recession methods that were used for  
 286 analysing the recession events of the three karst spring hydrographs. Only recession events  $\geq 7$  days period were considered  
 287 for analysis. For each spring hydrograph, a different number of recession events are extracted by the REMs. As shown on  
 288 Table 4, Vogel has the highest number of extracted recession events across all springs, followed by Brutsaert and Aksoy shows



289 least ability to capture recession events of the observed spring discharges. With this, the REMs can be simply classified as  
 290 permissive (Vogel), less permissive (Brutsaert) and restrictive (Aksoy).

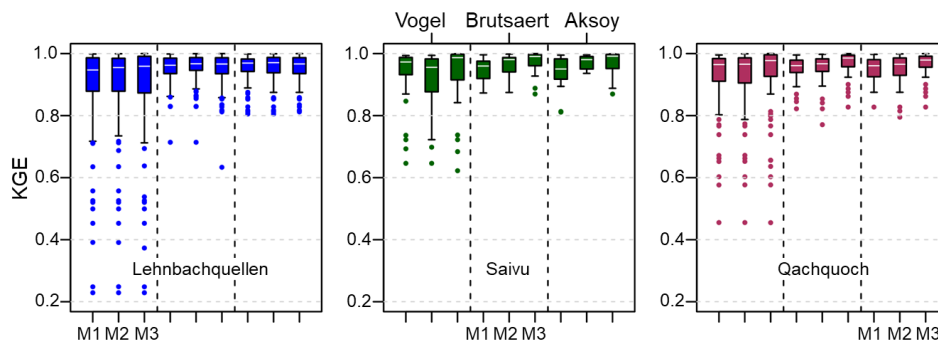
291

292 Table 4: Recession events period extracted by the REMs for the three spring discharge hydrograph

Spring name	Location	Catchment description	Number of extracted recession events		
			Vogel	Brutsaert	Aksoy
Lehnbachquellen	Austria	Snow dominated	162	145	136
Saivu	Switzerland	Humid	30	28	13
Qachquoch	Lebanon	Mediterranean	67	63	49

293

294 Figure 3 shows how the different REMs and POAs combinations performed in simulating spring discharge during extracted  
 295 recession events using KGE measures. With exclusion of the outliers, a high KGE values were achieved across all  
 296 combinations, ranging between 0.72 and 1.00. More than half of all simulated events across the three springs produce a KGE  
 297 >0.9 for all REM-POA pairs. However, the lowest performance in all three springs is related to POAs combined with Vogel  
 298 extraction method. While there is no vivid observable pattern between the extraction methods (REMs) and recession model  
 299 performance, the parameters optimisation approaches (POAs) show otherwise. A clear systematic order for the KGE median  
 300 is found within the POAs: M1 < M2 < M3. This is more noticeable in the humid and Mediterranean springs, except for the  
 301 Vogel-M2 combination in the humid spring that is not in the systematic order.



302

303

304



305 Figure 3: Boxplot of KGE measures between observed and simulated recession events based on parameters derived from the different REMs  
306 and POAs. The boxplots represent the interquartile ranges of KGE with the median shown in white lines and outliers marked in coloured  
307 points.

#### 308 4.2 Variability of recession parameters among different REM-POA combinations

309 Figure 4 shows the results of optimised recession parameters values with the different REM-POA pairs for each spring. These  
310 parameter sets are combinations of  $\alpha$ ,  $\eta$  and  $\varepsilon$  that produced the best simulation fit, that is highest KGE value for each recession  
311 event. Recession curve fitting based on the individual segment led to a large number of parameter combinations with the nine  
312 possible REM-POA pairs. Modification of REMs and POAs produce complex parameter interaction, to simplify the results,  
313 two categories of parameters were identified; (1) more consistent and less variable parameter ( $\alpha$ ); and (2) inconsistent  
314 parameter ( $\eta$  and  $\varepsilon$ ) with higher variability. However, this does not imply that, a parameter always falls into defined category  
315 for all pairs of REM and POA.

316 The results in Figure 4 shows that POAs do not have a noticeable influence on the estimation of recession coefficients  $\alpha$ .  
317 However, the REM has some impacts, which is only noticeable for Saivu and Qachquoch springs. For these springs, estimation  
318 associated with Aksoy extraction method shows less variability and gives a lower value of  $\alpha$ . Results obtained from POAs  
319 paired Vogel and Brutsaert are within similar ranges but are slightly higher. Generally, there is relatively high consistency  
320 among REM-POA pairs in estimating  $\alpha$  for each spring, as shown by the median and mean values. In fact, there is much higher  
321 variability in estimated  $\alpha$  among recession events than the different REM-POA combinations. However, there is much higher  
322 consistency and lesser variability in  $\alpha$  estimated for Lehnbachquellen compare to the other two spring locations. Also, when  
323 compare to other parameters, there is often lesser variability in estimated  $\alpha$  among extracted events and parameters optimisation  
324 approaches.

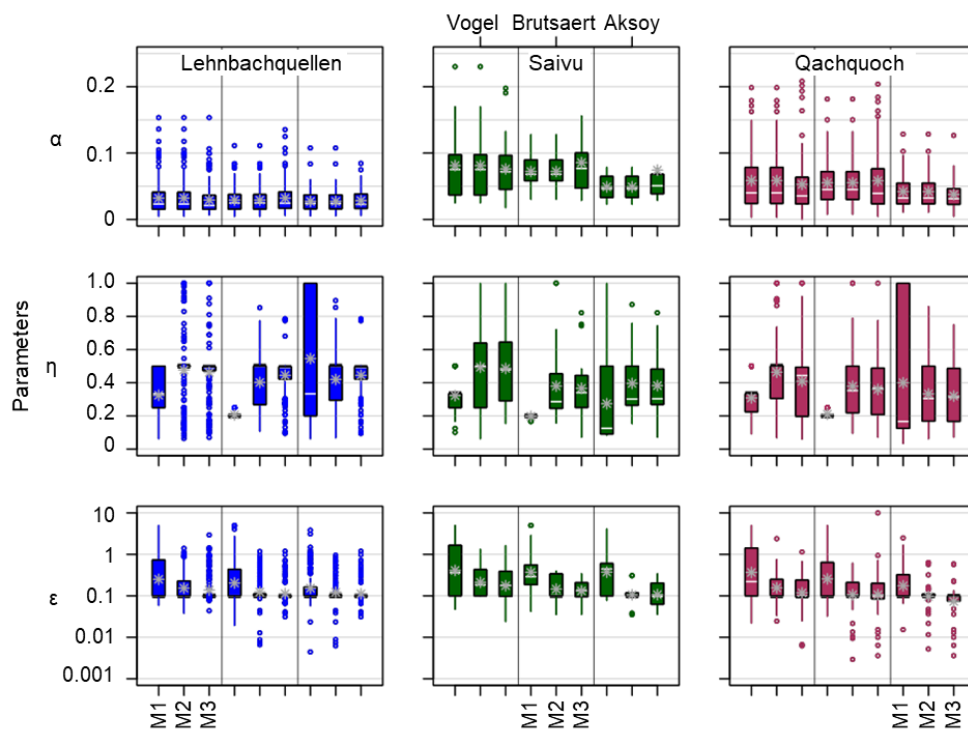
325

326 Both REM and POA have significant influence on the estimated values of infiltration rate,  $\eta$ , and curve concavity,  $\varepsilon$ ,  
327 parameters. Both parameters show relatively high inconsistency among the methods as well as instability within recession  
328 events. The most visible pattern from Figure 4 is that increasing degree of parameter freedom during optimisation usually  
329 result to higher estimates of  $\eta$  and vice-versa for parameter  $\varepsilon$ . The values of  $\eta$  parameter span one order of magnitude for REMs  
330 and POAs combinations across all spring locations. From the median and mean values, low estimates of  $\eta$  are related to pairing  
331 permissive extraction method (Vogel) with less-flexible optimisation approach (M1). Conversely, pairing the permissive  
332 extraction method with M2 and M3 which are more flexible optimisation approaches led to higher infiltration rates. Notably,  
333 a stationarity of  $\eta$  around  $0.2d^{-1}$  is seen across all springs with Brutsaert-M1 pairs. Unexpectedly, estimation of  $\eta$  with the  
334 restrictive extraction method (Aksoy) generally led to higher variability especially when combined with the less-flexible  
335 optimisation approach.

336



337 Estimation of curve concavity parameter,  $\varepsilon$ , with the different REM-POA combinations shows parameter behaviour opposite  
338 to that seen in the infiltration rate parameter. Pairing REMs with less-flexible optimisation procedure (M1) gives higher  
339 estimate of  $\varepsilon$ , yet the median and mean values derived from REM-POA pairs for each spring show some consistency. This  
340 consistency is higher for REMs paired with M2 and M3 optimisation approaches. While there are some coherency within  
341 REM-POA combinations, there is high variability in  $\varepsilon$  estimated for individual recession events. However, a significant  
342 reduction in the variability among recession events is seen with increasing restrictiveness of REM and more flexibility of POA.  
343 Overall, permissive REM and less-flexible POA result in slightly higher values and more variability in  $\varepsilon$  parameter estimates.  
344  
345



346

347 Figure 4. Distribution and variability of recession parameters  $\alpha$ ,  $\eta$  and  $\varepsilon$  (y-axis of  $\varepsilon$  in log scale, all units in  $\text{day}^{-1}$ ) obtained by  
348 the combination of REM (Vogel, Brutsaert and Aksoy) and POA (M1, M2 and M3) for the three springs located in the different



349 defined climate catchments. The boxplots represent the interquartile range, whisker lines correspond to the most extreme  
350 parameter values and outliers marked as circle with corresponding box colour.

351

### 352 4.3 Aquifer characterization

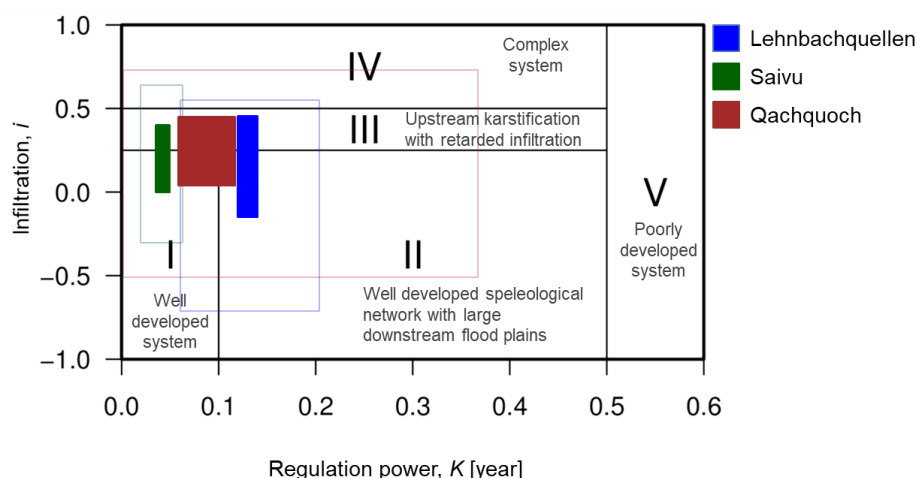
353 To evaluate the overall representativeness of estimated recession parameters based on the modified REMs and different POAs  
354 for the selected karst spring systems, we determined the drainage properties of the spring's aquifer using the parameters derived  
355 from the individual recession event. As described in subsection 2.2, retardation between infiltration and output defined by  
356 infiltration delay parameter,  $i$  and aquifer regulation power,  $K$ , were calculated for individual recession event. Figure 5 shows  
357 the grouped mean aquifer classifications as well as their standard deviations based on the per event  $K$  and  $i$  values, using the  
358 nine possible REM-POA combinations. Event-based estimated  $K$  and  $i$  values and their variability with respect to recession  
359 analysis methods are provided in the appendix (Figure A1). As shown by the standard deviation bounds of the drainage  
360 properties derived from individual recession segments in Figure 5, there is strong overlapping of calculated drainage properties  
361 and aquifer classes. However, with the calculated mean values of  $K$  and  $i$ , the three springs are identified as a distinct aquifer  
362 system. The aquifer systems are mostly distinguishable by their ability to store and regulate groundwater outflow through the  
363 springs.

364

365 With the exception of Qachquoch spring, there is high coherency for the mean  $K$  determined by the possible combinations of  
366 REM and POA for each springs. Conversely, methodological differences in selected REM and POA result in large variations  
367 in the estimated mean infiltration delay,  $i$ , among the springs. Lehnbachquellen spring located in snow-dominated catchment  
368 has a unanimous mean  $K$  of ca. 0.11 year and  $i$  values ranging from 0 to 0.4. The range covered by  $i$  is wide, yet most of the  
369 REM-POA combinations categorise the karst aquifer drained by Lehnbachquellen as speleologically well developed (class II)  
370 system. The only exception found was the Vogel-M1 paring, in which the system is ranked as fairly karstified (class III) (see  
371 Figure A1). Similarly, mean  $K$  value for the Saivu spring is also consistent across different extraction and parameter  
372 optimisation methods. The estimated mean  $K$  for the spring's karst system is 0.04 years while the mean infiltration delay,  $i$ ,  
373 ranges between 0 and ca. 0.35. Unlike Lehnbachquellen, there is no predominant classification established by the different  
374 REM-POA combinations. The Saivu karst spring system is placed between very well developed (class I) and fairly karstified  
375 systems (class III). In contrast to the other two springs, there is no unanimous agreement between the combinations of REM  
376 and POA in the estimation of the mean regulation capacity,  $K$ , of the Qachquoch spring system. Extraction with Vogel and  
377 Brutsaert methods combined with M3 parameterisation procedure result in a significant departure from the mean  $K$  values  
378 calculated by other REM-POA pairs. The capacity of the Qachquoch karst spring's aquifer to withhold water within the system  
379 ranges between 0.06 and 0.11 years (range of mean  $K$  values). But in a similar trend to other springs, wide dispersion is also



380 seen in the estimated mean infiltration delay,  $i$ , values which ranges from 0 to 0.4. Again, a decisive system class cannot be  
381 assigned, although most of the methods combination described the system as fairly karstified with retarded infiltration (class  
382 III). Classification of the aquifer system based on drainage characteristics ( $K$  and  $i$ ) calculated by Brutsaert-M2 and Aksoy-  
383 M1 pairs categorized it as well-developed (class I) system (see Figure A1).  
384



385  
386

387 Figure 5. Karst aquifer type classification based on mean values of  $K$  and  $i$ , calculated with recession parameters estimated by the different  
388 combinations of REM and POA. Distributions of mean  $K$  and  $i$  derived from all method combinations for each spring are represented by  
389 coloured areas; areas covered by unfilled boxes are the standard deviations. Mean and standard deviations  $K$  and  $i$  from different pairs of  
390 REM and POA for each spring are plotted in Fig. A1 of the appendix.

## 391 5 Discussion

### 392 5.1 Quality of extracted recessions

393 With the modification of the traditional REMs, we are able to establish a completely objective approach to distinguish between  
394 slow and quick flow recession components. Furthermore, optimisation approaches (POAs) with more flexibility show better  
395 improvement over the conventional parametrisation procedure. The REMs tested uses different statistical indices to scrutinise  
396 genuine baseflow records, hence they have different level of tolerance. The ability of the extraction methods to identify  
397 recession periods from hydrograph time series depend on the level of their restrictiveness. Vogel extraction method defined  
398 by a 3-day moving average to smoothen the hydrograph and also allows for 30% increase in subsequent flowrates is more  
399 permissive than Brutsaert and Aksoy methods that strictly enforce  $dQ/dt < 0$ . Hence, more recession events are extracted by  
400 Vogel method. Study by Stoelzle et al. (2013) also showed the Vogel procedure to be more permissive, as it was able extract  
401 almost 50% more events than Brutsaert. Although main recession selection condition for Brutsaert and Aksoy method is





402 determined by decreasing  $dQ/dt$ , constraining real baseflow recessions to discharge data points with less than 10% ( $CV \leq 0.1$ )  
403 deviations makes the Aksoy more restrictive than Brutsaert method.

404

405 Generally, all combinations of REM-POA performed acceptably well, increasing restrictiveness of extraction method gave  
406 improved model performance. Even though restrictiveness led to better performance, this should not be a basis to out-rightly  
407 accept restrictive REM over less-restrictive one. For instance, standard removal of 3 or 4 days by Brutsaert method as  
408 stormflow-influenced period is speculative and consequently led to unrealistic stationarity in conduit flow duration,  $t_i$ , ( $t_i = 1/\eta$ ),  
409 yet it performed better than permissive Vogel method. Although, problem of unrealistic  $t_i$  estimation inherent from Brutsaert  
410 was eliminated and general improvement in models performance was achieved by increasing parameters flexibility during  
411 optimisation. Overall, the adapted REMs and the introduced three POAs provide range of results that adequately represents  
412 the karst systems. This suggests that the modified REMs are well suited for application to karst spring recession analysis.  
413 While all REM-POA pairs are good from the model performance perspective, it will be misleading to define best pair of REM-  
414 POA base on this, without first evaluating if the estimated parameters are realistic. However, we strongly suggests avoiding  
415 the Brutsaert-M1 pair for karst recession analysis due to its stationarity problem.

#### 416 **5.2 Effects of different REM-POA combinations on extracted recession parameters**

417 Methodological choices of REMs and POAs combinations have great impacts on the estimated recession parameters. The  
418 extent to which the parameters are influenced by the methods largely varies between the slow flow and quick flow recession  
419 parameters. There is relatively higher consistency and better stability among all REM-POA pairs in estimating slow flow  
420 recession parameter that describe the drainage characteristics of the matrix block within the phreatic zone. As observed by few  
421 other studies (Stoelzle et al. 2013; Santos et al. 2019) slow flow recession coefficient is more influenced by the extraction  
422 method used than the parameterisation approach, which only marginally impacts the estimated parameter. The heterogeneity  
423 of karst system results in different conduit processes being activated during recharge events, this is reflected in observed higher  
424 variability of quick flow parameters that represent the conduit drainage system. Unlike slow flow parameter, both REM and  
425 POA greatly impacted the estimation of parameters representing the conduit drainage systems.

426

427 More variability in estimated recession parameters is largely associated with analysis involving permissive extraction method,  
428 though increasing flexibility of model parameterisation often reduced the variability. Such large variability was also reported  
429 by Santos et al. (2019) who suggested avoiding combining the permissive extraction method with individual recession segment  
430 analysis to estimate recession parameters. Aside showing higher variability, permissive recession extraction tends to produce  
431 higher estimate of slow flow recession coefficients. However, as seen from Lehnbachquellen spring in snow-dominated  
432 catchment where outflow is generously sustained throughout the year without seasonality of baseflow regimes, all REMs



433 produced very similar estimate of baseflow coefficients with narrow variability. The more variability and over-estimation of  
434 slow flow recession coefficients by permissive and less-permissive REMs (Vogel and Brutsaert) as early mentioned is  
435 specifically noticeable only for springs in the humid or mediterranean catchments. This observation suggests that the impact  
436 of methodological difference of various REMs associated with estimated baseflow parameters might only be pronounced in  
437 catchments with hydrological seasonality.

438

439 Although the combination of REM and POA affects the estimation of conduit drainage characteristics, the effect of the POA  
440 tends to be more pronounced. Increasing degree of parameter freedom during optimisation with the different POAs  
441 formulations often result to significant reduction in parameters variability. This is also accompanied by either over- or under-  
442 estimation of conduit drainage parameters. The more flexible parameterisation approaches (M2 and M3) generally lead to  
443 higher the infiltration rates through the unsaturated zone. Infiltration rate is predetermined ( $\eta = 1/t_i$ ) in the original  
444 parameterisation procedure of Mangin's model (M1) which restricts fitting the quick flow recession curve only to the  
445 optimisation of the regulating capacity,  $\varepsilon$ . To compensate the inflexibility due to predetermined infiltration rate, the regulation  
446 capacities of the reservoir estimated with M1 parameterisation procedure are higher and more varied. By means of excluding  
447 a fixed number of days (3-4) as influenced stage of recession, Brutsaert paired with M1 also leads to stationarity in the  
448 estimated infiltration rates. This makes it an unsuitable combination, especially with long recession period. Santos et al. (2019)  
449 found analysis with Brutsaert method to be more robust and appropriate for short recession samples.

450 Despite the impacts of methodological choices on the uncertainty of estimated recession parameters, variability among events  
451 exceed the variability among methods. These high variabilities are attributed to different lengths of extracted recession events,  
452 differences in karstic processes such as recharge and infiltration that are activated within the unsaturated zone for each event.  
453 Even though karst systems are very heterogeneous and it is important to capture the impacts of the variable karstic processes  
454 through analysis of individual recession segment, the high uncertainty among events make it difficult to define set of  
455 representative recession parameters. This uncertainty found with per event analysis can be reduced by considering different  
456 categories of recession lengths that represent short and long recession periods; estimated parameters can be compared to assess  
457 the system's dynamics. Another way of coping with this problem is to consider master recession curve analysis which is often  
458 criticize for its inability to adequately represent storage variability (Kresic and Bonacci 2010; Gregor and Malík 2012; Kovacs  
459 2021). However, since per event analysis is useful for better understanding of the system's dynamic, defining a systematic  
460 approach to quantify parameters uncertainty will help to increase the confidence of individual recession segment analysis.

### 461 **5.3 How realistic are adapted REM-POA for karst system analysis?**

462 Interestingly, there is a strong coherence among possible pairs of REM and POA in determining the average regulation capacity  
463 of the aquifers drained by the springs. The determination of the dynamic volume used in calculating the regulation capacity is



464 based on baseflow recession coefficients (Eq. 6). However, the effect of the extraction methods on baseflow recession  
465 coefficient (see previous sub-section) was not reflected in the determination of dynamic volume and regulation power. This  
466 effect that could have been transmitted was cancelled by different initial baseflow component,  $Q_{r0}$ , estimated by the methods.  
467 In one study (Grasso & Jeannin 1994), the authors found regulation power,  $K$ , to be more stable for various years and events.  
468 These findings do not agree with our analysis, the outcomes of which show a large variability among  $K$  for different events,  
469 most significantly in the snow-dominated catchment (Figure A1 in Appendix). Regulation power is analogous to memory  
470 effect, periodic water release from an external snow storage that is not captured within the saturated zone in real time makes  
471  $K$  to fluctuate more in snow-dominated catchment.

472

473 Infiltration delay,  $i$ , is strongly dependent on recharge type contribution as well as catchment size (Jeannin and Sauter 1998).  
474 Pairing extraction method that does not explicitly separate the spring discharge slow and fast recharge path (Brutsaert) with  
475 less flexible parameterisation procedure (M1) result in overestimation of infiltration delay. Aside this obvious bias with  
476 Brutsaert-M1 pairs, regardless of what extraction method (permissive or restrictive) is paired with parameterisation procedure,  
477 the complex interplay of REM and POA result in a compensation phenomenon; whereby infiltration rate,  $\eta$ , is compensated  
478 by recession concavity parameter,  $\varepsilon$ , and vice versa. Since the infiltration delay, is defined by these parameters, it is difficult  
479 to explicitly infer specific effect of REM and POA on infiltration delay.

480

481 The northern Alps karst system where the Lehnbachquellen spring is located has been defined as well karstified highly  
482 permeable unit interlayered with less permeable Flysch formation (Goldscheider 2005; Chen et al. 2018). This is very  
483 consistent with the classification we achieved (class II and III). Perrin, Jeannin, & Zwahlen (2003) described Saivu spring  
484 system as a well-developed karstic network, majority of the methods pair used in this study place this spring in class 1, therefore  
485 coherently agreeing with the authors description. From our analysis, Qachquoch spring is classified as medium karstified  
486 system by most method combinations. However recent study by Dubois et al. (2020) categorise the system as poorly karstified  
487 with a very large regulation capacity. Meanwhile, if we also consider two standard deviation distances from the calculate mean  
488  $K$  values, a regulation capacity  $>0.5$  will be obtained and the system will be equally classified as poorly karstified by REM-  
489 POA pairs used.

490

491 Given that existing common karst spring recession extraction method involves manual procedure and subjectively determined  
492 duration of conduit infiltration, alternative faster, automated and objective approach is very useful. From our analysis, resulting  
493 parameters of extracted recession segments are within reasonable ranges and derived systems classification correspond to those  
494 found in literatures. The good performance recorded between simulated and observed flowrates during recession events attest  
495 to the potential transferability of traditional extraction methods to karst systems. However, this good performance does not



496 necessarily translate to reliable parameter estimates. It is therefore important to choose REM methods that gives reasonable  
497 parameters especially when paired with a less flexible optimisation approach. Furthermore, with prior knowledge of the spring  
498 system, parameters ranges can be reasonably constrained during optimisation to achieve a more representative optimum  
499 parameters.

## 500 **6 Conclusions**

501 The application of karst spring hydrographs recession analysis is very broad, including estimation of storage capacity (Fleury  
502 et al. 2007), describing discharge of unsaturated zone (Amit et al. 2002; Mudarra and Andreo 2011) as well as systems  
503 classification (El-Hakim and Bakalowicz 2007). Most often manual recession extraction is used and the high subjectivity of  
504 the approach introduces bias to estimated parameters. For the first time in literatures, this study explores the applicability of  
505 automated traditional recession extraction methods (REMs) originally developed for slow flow (baseflow) recession by  
506 adapting them to also identify quick flow flow recessions. We fit individual extracted recession segments with Mangin's  
507 recession model to determine the conduit and matrix drainages recession characteristics. We introduce new parameters  
508 optimisation approaches (POAs) different from the conventional procedure to increase degree of freedom of parameter  
509 interaction.

510

511 The three traditional REMs adapted in this study performed differently, depending on how permissive or constraining the  
512 method was, more or less recession periods were identified. The interaction between REMs and POAs is complex and has  
513 various degree of impacts on the derived recession parameters. We found that higher variability is associated with permissive  
514 extraction method but this variability is largely reduced with an increased degree of freedom during optimisation. Unlike with  
515 baseflow conditions, where estimated recession parameters are a bit consistent among REMs and POAs, there is high  
516 variability for the estimated conduit recession parameter. However, parameters variability among individual recession events  
517 exceed the variability resulting from different combinations of REM and POA. The original REMs were developed based on  
518 specific catchment features that control recession (Stoelzle et al. 2013), so they quantify recession extraction differently. As  
519 suggested in several recession studies (Stoelzle et al. 2013; Santos et al. 2019) and also done in this study, we recommend  
520 trying different combinations of REMs-POAs for more robust recession analysis.

521

522 The adapted traditional REMs tested produced reasonable results with regard performance and derived parameters. Application  
523 of the methods is quick and fully objective, therefore they proved to be a good alternative to manual recession extraction. This  
524 will be useful for the comparative analysis of karst spring systems using large number of hydrographs which would otherwise  
525 be a difficult exercise to execute. Although analysis with individual recession events is highly uncertain, we provide alternative  
526 for reducing or quantifying the uncertainties to improve the robustness of the analysis.



527

528 *Acknowledgements.* Support to T.O. and A.H was provided by the Emmy Noether Programme of the German Research  
529 Foundation (DFG; grant no. HA 8113/1-1; project “Global Assessment of Water Stress in Karst Regions in a Changing  
530 World”).

### 531 **References**

- 532 Aksoy H, Wittenberg H (2011) Nonlinear baseflow recession analysis in watersheds with intermittent streamflow. *Hydrol Sci*  
533 *J* 56:226–237. <https://doi.org/10.1080/02626667.2011.553614>
- 534 Amit H, Lyakhovskiy V, Katz A, et al (2002) Interpretation of Spring Recession Curves. *Ground Water* 40:543–551.  
535 <https://doi.org/10.1111/j.1745-6584.2002.tb02539.x>
- 536 Arciniega-Esparza S, Breña-Naranjo JA, Pedrozo-Acuña A, Appendini CM (2017) HYDRORECESSION: A Matlab toolbox  
537 for streamflow recession analysis. *Comput Geosci* 98:87–92. <https://doi.org/10.1016/j.cageo.2016.10.005>
- 538 Atkinson T. (1977) DIFFUSE FLOW AND CONDUIT FLOW IN LIMESTONE TERRAIN IN THE MENDIP HILLS,  
539 SOMERSET (GREAT BRITAIN). *J Hydrol* 35:93–110
- 540 Beck HE, Zimmermann NE, Mcvicar TR, et al (2018) Data Descriptor: Present and future Köppen-Geiger climate  
541 classification maps at 1-km resolution. <https://doi.org/10.1038/sdata.2018.214>
- 542 Bonacci O (1993) Karst springs hydrographs as indicators of karst aquifers. *Hydrol Sci J* 38:51–62.  
543 <https://doi.org/10.1080/02626669309492639>
- 544 Brutsaert W (2008) Long-term groundwater storage trends estimated from streamflow records: Climatic perspective. *Water*  
545 *Resour Res* 44:. <https://doi.org/10.1029/2007WR006518>
- 546 Chen Z, Hartmann A, Wagener T, Goldscheider N (2018) Dynamics of water fluxes and storages in an Alpine karst catchment  
547 under current and potential future climate conditions. *Hydrol Earth Syst Sci* 22:3807–3823. [https://doi.org/10.5194/hess-](https://doi.org/10.5194/hess-22-3807-2018)  
548 [22-3807-2018](https://doi.org/10.5194/hess-22-3807-2018)
- 549 Civita M V, Civita M V (2008) An improved method for delineating source protection zones for karst springs based on analysis  
550 of recession curve data. *Hydrogeol J* 16:855–869. <https://doi.org/10.1007/s10040-008-0283-4>
- 551 Dewandel B, Lachassagne P, Bakalowicz M, et al (2003) Evaluation of aquifer thickness by analysing recession hydrographs.  
552 Application to the Oman ophiolite hard-rock aquifer. *J Hydrol* 274:248–269. [https://doi.org/10.1016/S0022-](https://doi.org/10.1016/S0022-1694(02)00418-3)  
553 [1694\(02\)00418-3](https://doi.org/10.1016/S0022-1694(02)00418-3)
- 554 Dubois E, Doummar J, Pistre S, Larocque M (2020) Calibration of a lumped karst system model and application to the  
555 Qachqouch karst spring (Lebanon) under climate change conditions. *Hydrol Earth Syst Sci* 24:4275–4290.  
556 <https://doi.org/10.5194/hess-24-4275-2020>
- 557 El-Hakim M, Bakalowicz M (2007) Significance and origin of very large regulating power of some karst aquifers in the Middle



- 558 East. Implication on karst aquifer classification. *J Hydrol* 333:329–339. <https://doi.org/10.1016/j.jhydrol.2006.09.003>
- 559 Fandel C, Ferré T, Chen Z, et al (2020) A model ensemble generator to explore structural uncertainty in karst systems with  
560 unmapped conduits. *Hydrogeol J*. <https://doi.org/10.1007/s10040-020-02227-6>
- 561 Fiorillo F (2014) The Recession of Spring Hydrographs, Focused on Karst Aquifers. *Water Resour Manag* 28:1781–1805.  
562 <https://doi.org/10.1007/s11269-014-0597-z>
- 563 Fiorillo F (2011) Tank-reservoir drainage as a simulation of the recession limb of karst spring hydrographs. *Hydrogeol J*  
564 19:1009–1019. <https://doi.org/10.1007/s10040-011-0737-y>
- 565 Fleury P, Plagnes V, Bakalowicz M (2007) Modelling of the functioning of karst aquifers with a reservoir model: Application  
566 to Fontaine de Vaucluse (South of France). *J Hydrol* 345:38–49. <https://doi.org/10.1016/j.jhydrol.2007.07.014>
- 567 Ford D, Williams P (2007) *Karst Hydrogeology and Geomorphology*. John Wiley and Sons, Ltd
- 568 Goldscheider N (2015) Overview of Methods Applied in Karst Hydrogeology. In: Stevanović Z (ed) *Karst Aquifers---*  
569 *Characterization and Engineering*. Springer International Publishing, Cham, pp 127–145
- 570 Goldscheider N (2005) Fold structure and underground drainage pattern in the alpine karst system Hochifen-Gottesacker.  
571 *Eclogae Geol Helv* 98:1–17. <https://doi.org/10.1007/s00015-005-1143-z>
- 572 Goldscheider N, Chen Z, Auler AS, et al (2020) Global distribution of carbonate rocks and karst water resources
- 573 Goldscheider N, Drew D (2007) *Methods in Karst Hydrogeology*. International Contributions to Hydrogeology 26,  
574 International Association of Hydrogeology. Taylor & Francis, London
- 575 Goldscheider N, Neukum C (2010) Fold and fault control on the drainage pattern of a double-karst-aquifer system,  
576 winterstaude austrian alps. *Acta Carsologica* 39:173–186. <https://doi.org/10.3986/ac.v39i2.91>
- 577 Gregor M, Malík P (2012) Construction of master recession curve using genetic algorithms. *J Hydrol Hydromechanics* 60:3–  
578 15. <https://doi.org/10.2478/v10098-012-0001-8>
- 579 Gupta H V., Kling H, Yilmaz KK, Martinez GF (2009) Decomposition of the mean squared error and NSE performance  
580 criteria: Implications for improving hydrological modelling. *J Hydrol* 377:80–91.  
581 <https://doi.org/10.1016/j.jhydrol.2009.08.003>
- 582 Hartmann A, Mudarra M, Andreo B, et al (2014) Modeling spatiotemporal impacts of hydroclimatic extremes on groundwater  
583 recharge at a Mediterranean karst aquifer. *Water Resour Res* 1–15. <https://doi.org/10.1002/2014WR015685>
- 584 Hartmann A, Weiler M, Wagener T, et al (2013) Process-based karst modelling to relate hydrodynamic and hydrochemical  
585 characteristics to system properties. *Hydrol Earth Syst Sci* 17:3505–3521. <https://doi.org/10.5194/hess-17-3305-2013>
- 586 Jachens ER, Rupp DE, Roques C, Selker JS (2020) Recession analysis revisited: impacts of climate on parameter estimation.  
587 *Hydrol Earth Syst Sci* 24:1159–1170. <https://doi.org/10.5194/hess-24-1159-2020>
- 588 Jeannin P-Y, Sauter M (1998) Analysis of karst hydrodynamic behaviour using global approaches: a review
- 589 Kiraly L (2003) Karstification and Groundwater Flow. *Speleogenes Evol karst aquifers* 1:155–192



- 590 Kovacs A (2021) Quantitative classification of carbonate aquifers based on hydrodynamic behaviour.  
591 <https://doi.org/10.1007/s10040-020-02285-w>
- 592 Kovács A, Perrochet P, Király L, Jeannin PY (2005) A quantitative method for the characterisation of karst aquifers based on  
593 spring hydrograph analysis. *J Hydrol* 303:152–164. <https://doi.org/10.1016/j.jhydrol.2004.08.023>
- 594 Kresic N, Bonacci O (2010) Spring discharge hydrograph
- 595 Larson EB, Mylroie JE (2018) Diffuse versus conduit flow in coastal karst aquifers: The consequences of Island area and  
596 perimeter relationships. *Geosci* 8:. <https://doi.org/10.3390/geosciences8070268>
- 597 Liu L, Shu L, Chen X, Oromo T (2010) The hydrologic function and behavior of the Houzhai underground river basin, Guizhou  
598 Province, southwestern China. *Hydrogeol J* 18:509–518. <https://doi.org/10.1007/s10040-009-0518-z>
- 599 Maillet E (1905) *Essais d'hydraulique souterraine et fluviale*. Hermann
- 600 Mangin A (1975) *Contribution à l'étude hydrodynamique des aquifères karstiques*. Institut des Sciences de la Terre de  
601 l'Université de Dijon
- 602 Mazzilli N, Guinot V, Jourde H, et al (2019) KarstMod: A modelling platform for rainfall - discharge analysis and modelling  
603 dedicated to karst systems. *Environ Model Softw* 122:103927. <https://doi.org/10.1016/j.envsoft.2017.03.015>
- 604 Mudarra M, Andreo B (2011) Relative importance of the saturated and the unsaturated zones in the hydrogeological  
605 functioning of karst aquifers: The case of Alta Cadena (Southern Spain). *J Hydrol* 397:263–280.  
606 <https://doi.org/10.1016/j.jhydrol.2010.12.005>
- 607 Olarinoye T, Gleeson T, Marx V, et al (2020) Global karst springs hydrograph dataset for research and management of the  
608 world's fastest-flowing groundwater. *Sci Data* 2020 71 7:1–9. <https://doi.org/10.1038/s41597-019-0346-5>
- 609 Padilla A, Pulido-Bosch A, Mangin A (1994a) Relative Importance of Baseflow and Quickflow from Hydrographs of Karst  
610 Spring. *Ground Water* 32:267–277
- 611 Padilla A, Pulido-Bosch A, Mangin A (1994b) Relative Importance of Baseflow and Quickflow from Hydrographs of Karst  
612 Spring. *Ground Water* 32:267–277. <https://doi.org/10.1111/j.1745-6584.1994.tb00641.x>
- 613 Perrin J, Jeannin PY, Zwahlen F (2003) Implications of the spatial variability of infiltration-water chemistry for the  
614 investigation of a karst aquifer: A field study at Milandre test site, Swiss Jura. *Hydrogeol J* 11:673–686.  
615 <https://doi.org/10.1007/s10040-003-0281-5>
- 616 Santos AC, Portela MM, Rinaldo A, Schaepli B (2019) Estimation of streamflow recession parameters: New insights from an  
617 analytic streamflow distribution model. *Hydrol Process* 1–15. <https://doi.org/10.1002/hyp.13425>
- 618 Schuler P, Duran L, Johnston P, Gill L (2020) Quantifying and numerically representing recharge and flow components in a  
619 karstified carbonate aquifer. *Water Resour Res*. <https://doi.org/10.1029/2020wr027717>
- 620 Sivellev V (2020) A methodology for the assessment of groundwater resource variability in karst catchments with sparse  
621 temporal measurements



- 622 Stevanović Z (2018) Global distribution and use of water from karst aquifers. In: Geological Society Special Publication.  
623 Geological Society of London, pp 217–236
- 624 Stoelzle M, Stahl K, Weiler M (2013) Are streamflow recession characteristics really characteristic? Hydrol Earth Syst Sci  
625 17:817–828. <https://doi.org/10.5194/hess-17-817-2013>
- 626 Vogel RM, Kroll CN (1996) Estimation of Baseflow Recession Constants. Kluwer Academic Publishers
- 627 Vogel RM, Kroll CN (1992) Regional geohydrologic-geomorphic relationships for the estimation of low-flow statistics. Water  
628 Resour Res 28:2451–2458. <https://doi.org/10.1029/92WR01007>
- 629 WMO (2008a) Manual on Low-flow Estimation and Prediction : Operational Hydrology Report No.50
- 630 WMO (2008b) Guide to Meteorological Instruments and Methods of Observation
- 631 Xu B, Ye M, Dong S, et al (2018) A New Model for Simulating Spring Discharge Recession and Estimating Effective Porosity  
632 of Karst Aquifers A new model for simulating spring discharge recession and estimating effective porosity of karst  
633 aquifers. J Hydrol 562:609–622. <https://doi.org/10.1016/j.jhydrol.2018.05.039>
- 634
- 635
- 636
- 637
- 638
- 639
- 640
- 641
- 642
- 643
- 644
- 645
- 646
- 647
- 648
- 649
- 650
- 651
- 652
- 653
- 654
- 655





656 **Appendix**

657

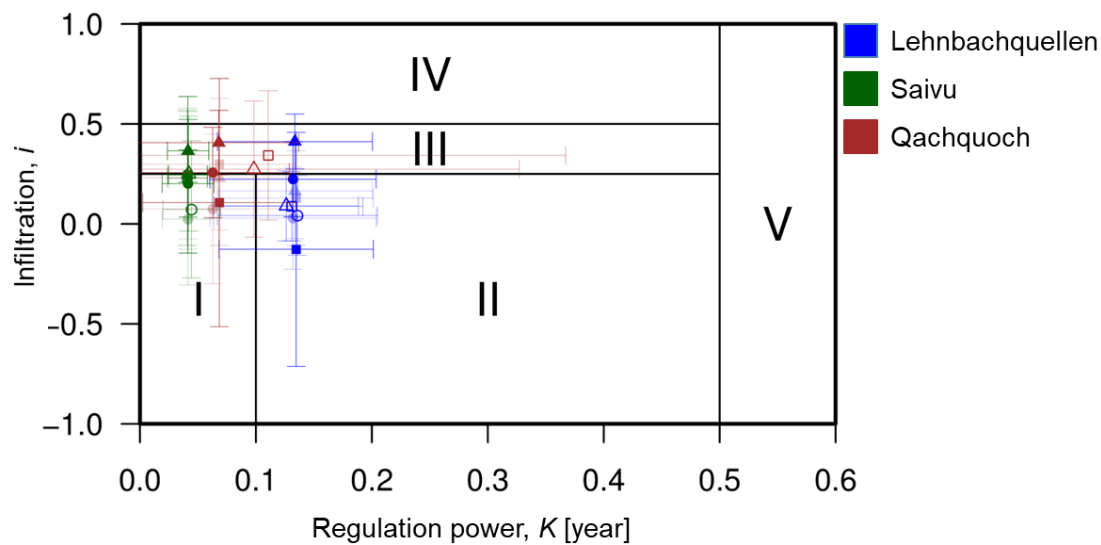
658 Table A1. Spearman's ranked correlation coefficients,  $\rho$ , between the recession parameters and length of extracted recession  
 659 events.

	vog_M1	vog_M2	vog_M3	brut_M1	brut_M2	brut_M3	akw_M1	akw_M2	akw_M3
?	-0.19673	-0.19673	-0.08805	-0.0918	-0.09191	-0.1215	-0.05995	-0.06002	0.045158
?	-0.9722	-0.55059	-0.31179	-0.14328	-0.47121	-0.29442	-0.62963	-0.63559	-0.35843
?	0.04843	0.05108	-0.0257	-0.16752	-0.0788	-0.03305	0.106504	-0.10938	-0.08331

660

661

662



663

664

665 Figure A1. Karst aquifer classification according to the different combinations of REMs and POAs. The shapes circle, triangle and square  
 666 represents (Vogel, Brutsaert and Aksoy) extraction methods. Different colour fills relate to parameterisation procedures; solid colour for  
 667 M1, transparent for M2 and no-fill for M3.

668

669

670

671

672

673

674